Performance Analysis of Satellite Tracking Algorithms in Low SNR Environments

James Helferty, Ph. D, Jennifer Smith, Edgar Ryan, Manual Thomas
KBR, Inc.

ABSTRACT

Algorithms that process multiple frames are critical for identifying dim satellites signals and orbital motion in wide area searches. Track Before Detect methods look at multiple images that have target signals and supply all the frame data to the tracker and delay the detection decision until the track is formed. This paper looks to estimate the performance of low SNR tracking algorithms by modeling a binomial decision rule over all frames. As part of the system engineering analysis, it is necessary to predict the performance of the of the search based on a variety of parameters such as aperture, transmission, detector sensitivity, number of frames, minimum detectable target size, attenuation, and other factors. The performance of these search algorithms can be determined by Monte Carle (MC) simulation which take many iterations to create tables to describe the expected system performance. Unfortunately, these predictions based on MC can require extensive rework when system parameters and target characteristics change leading to mission delays. This work looks to describe an analytic expression to describe the expected detection and false alarm performance of a scenario that will allow search and collection tasking of observing platforms in a Space Domain Awareness (SDA) mission. Alternatively, an analytic expression can directly describe these changes with greater initiative understanding of results and better understand any operational anomalies.

1. INTRODUCTION

In a wide area search scenario, a telescope must scan a wide volume of the sky, track known satellites, and identify unexpected and unknown objects. Multiple collections on a target area are necessary to help differentiate the star clutter from the moving satellite objects. This also allows for redundancy in the collection to help improve detection performance and remove false alarms using correlation among the frames [1]. This paper looks to estimate the performance of low SNR tracking algorithms by applying a binomial decision rule to model processing over all frames.

In a space-based search, the observer is at LEO and is staring at a region in the GEO-belt. The observing satellite will be pointing directly at a target GEO satellites which appear stationary with stars forming streaks due to its relative motion. The stars can be identified and removed by identifying the streak signature and correlation between sequential frames.

The satellite scans its search region using repetitive scans within its field of view. The search area is separated into bins based on the limited frames size of the field of view. The observing satellite will scan each bin for an RSO detection and move to the next to cover the area. An exhaustive search strategy will work through the field of regard to go back to the repeat the series for the next set of detections. The interval between RSO detection should be minimized to maintain consistent track on an RSO.

The paper describes a way to model the detection performance of the RSO over repeated collections. Multiple collections are utilized for detecting dim RSO's with minimal false alarms that could be present from stray stars or detector noise. The tracking algorithm will mitigate false alarms using multiple collections to correlate slowly moving RSOs in the GEO-belt and remove the other stray false alarms. The performance estimation is needed system engineering requirements development to compare constellation configuration, Field of view and resolution requirements, Aperture size, and processing techniques.

The first section of the paper will highlight the analysis methodology. Analysis will include estimating intensity level of the RSOs and stars into the aperture, telescope SNR modeling, and Receiver Operator Characteristic curves from single image and multiple image correlation with a tracker. A MATLAB simulation is used to compare the analytic curves to a Monte Carlo Simulation. The final section will review conclusions.

2. ANALYSIS OF DETECTION STATISTICS

2.1 Imaging Scenario

This paper considers a tracking problem where an observer satellite must track RSOs on a region of GEO-belt[2][3]. The observing sensor has a fixed field-of-view for each frame. The observer needs to scan the overall search space and quickly re-image tracks and maintain custody as shown in Fig. 1. The overall mission is a balance of search space, field-of-view, detection capability, agility, and tracking efficiency. Multiple collections are necessary in each bin to separate stars from collections and remove false alarms from dim collections.

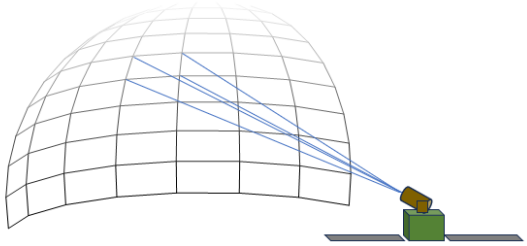

Fig 1. Image GEO belt scanning from LEO

The paper investigates analytical techniques to model the performance of the collection and tracking system that relies on multiple collections. The single image detection performance is based on the SNR of a single image. The false alarm performance is improved by correlating images over multiple collections.

An example image scenario can help illustrate the collection. This is based on a LEO satellite observer and a GEO RSO target in an example study from Vallado [4]. Fig 2 shows the orbit configuration in the STK tool. The LEO observer has a purple curve and the RSO at GEO has a green curve.

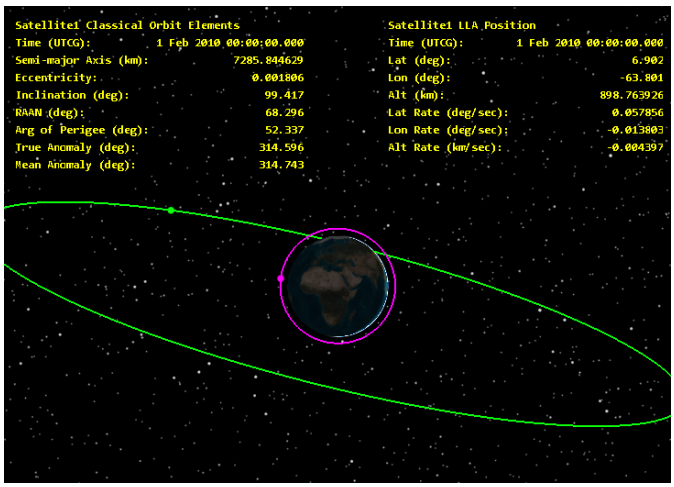

Fig 2. Example image scenario for RSO detection at GEO

A KBR image simulation tool called VINCI will be used to show a collection sequence at this geometry. The satellite and image parameters are shown in Table 1.

Table 1. Satellite observer parameters

Sensor Parameters	
Dimensions	1000x1000
Aperture	0.3m
Focal Length	5 m
Pitch	20 microns
Integration Time	1 sec
Wavelength	0.4-0.8 microns
Read Noise	60 electrons
Gimbal	2 axis

The observer will be pointing directly at the RSO target during collection. The scenario had 5 images taken with 1 second between frames. The images show the background stars moving as streaks in the image and the target is stationary in the image. Fig. 3 shows image number 1 and image number 4 in the sequence. There is a shift in the location of the stars and the target is in the center.

(a) 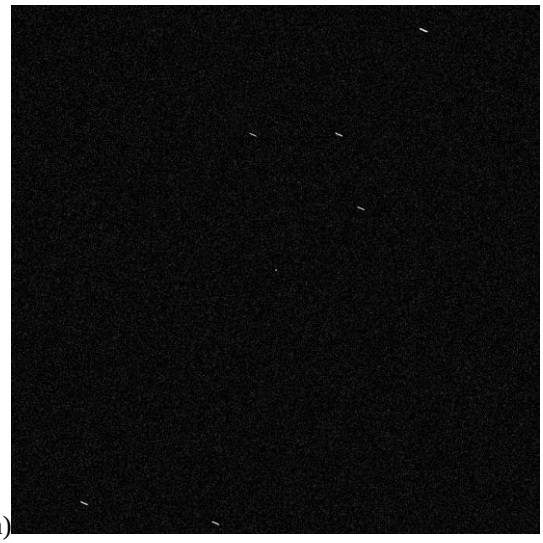 (b) 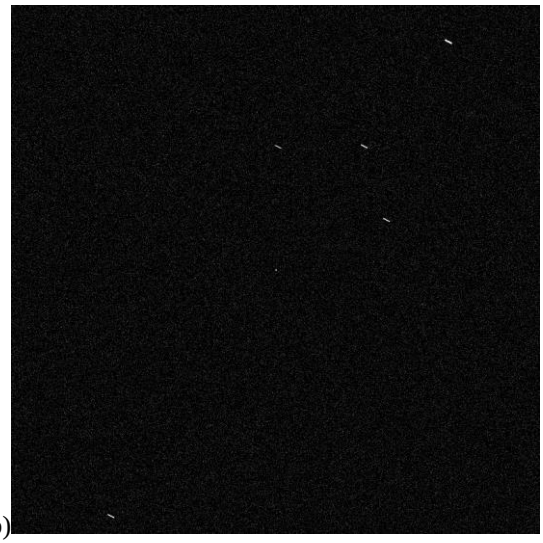

Fig. 3. Example image simulation of a LEO collection. (a) Image1 (b) Image 4

The stars are correlated between the successive scenes using a RANSAC [5] algorithm and identify their relative motion transformation. The remaining stars are processed as potential RSO collection. Resulting detections are shown in Fig. 4. The image on left shows the stars identified and removed from the detection set. There is a positive detection which is a target RSO in the center. The image on the right has the stars identified and removed. The target is detected in the center and there are 5 more stray detections. These would be processed by the tracking algorithm to determine if there are false alarms.

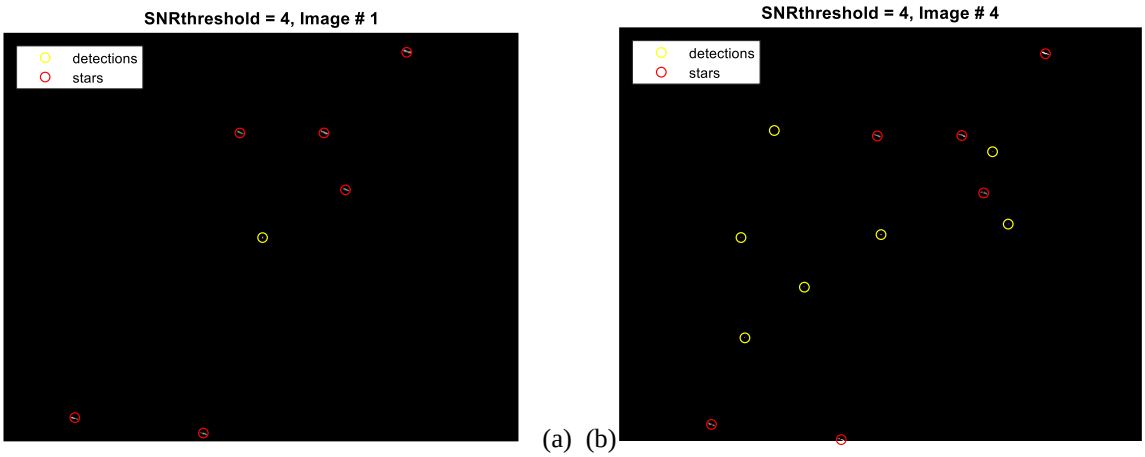

(a) (b)

Fig. 4. Star and Object detections (a) Image 1 (b) Image 4

The stars can be removed from the detection list. What remains are object detections and false alarms. It is possible to remove false alarms by correlating collections between images. The next sections show an estimate of the SNR based on target, geometry, and sensor parameter. Following that the detection statistics can be estimate from the single image case and for the case correlating between images.

2.2 Signal and Noise Level

The satellites are in the GEO-belt so are unresolved and their intensity is modeled using an apparent magnitude equation that models the satellite as a sphere. This apparent magnitude equation depends on the slant range, reflectance of the satellite, CATS angle and cross section area. The intensity of the signal from the satellite in Watts/m^2 can be calculated from the satellite Visual magnitude assuming the reflected follows the solar spectrum. This is the intensity immediately before the aperture.

It is convenient to capture the brightness of an unresolved satellite with the apparent magnitude formula for a spherical object to put the brightness in the equivalent visual magnitude scale,

$$m_v = -26.74 \; - 2.5 * \log\left(F_{diff}(\emptyset)\right)$$

$$F_{diff}(a_0, r_{sat}, \emptyset\,) = \frac{2}{3} * \rho * \frac{r_{sat}^2}{\pi R^2} * (\sin(\emptyset) + (\pi - \emptyset)\cos(\emptyset))$$

This formula assumes that r_{sat} is the radius of the object sphere, ϕ is the solar phase angle, R is the slant range, ρ is the material reflectance of the object.

Visual magnitude values given two brightness intensity values have the following scaling relationship,

$$\frac{B_1}{B_0} = 10^{-0.4(m_1 - m_0)}$$

where B_1 and B_0 are two measured intensities in w/m^2 and m_1 and m_0 are the corresponding visual magnitudes. We will assume these intensities are both in the sensor bandpass and the relationship holds.

If we can find the band limited brightness of Vega as B_0 with $m_0 = 0$, we can calculate the irradiance of any visual magnitude of the sensor according to the formula,

$$B_1 = Irr_{sen} = B_0 10^{-0.4 m_v}$$

Here $B_1 = Irr_{sen}$ is the irradiance into the aperture in w/m2 over the sensors bandpass. The B_0 constant allows the calculation of sensor irradiance given the visual magnitude of the object.

If we know the sensor bandpass, we can calculate the B_0 constant from the Sun's visual magnitude, solar spectrum, Total solar irradiance, and sensor response function. The visual magnitude of the sun is $m_{v,sun} = -26.74$. The solar spectral response from Planck's law at $T_{sun} = 5523K$ is calculated as

$$M_{sun}(\lambda) = \frac{2hc^2}{\lambda^5\left(\exp\left(\frac{hc}{\lambda k_B T_{sun}}\right) - 1\right)}$$

The fraction of the solar spectrum in the sensor bandpass, $SRF(\lambda)$ is calculated as

$$k_{sun} = \int_{\lambda 1}^{\lambda 2} M_{sun}(\lambda), SRF(\lambda)\, d\lambda \Big/ \int_{\lambda 1}^{\lambda 2} M_{sun}(\lambda)\, d\lambda$$

Given total irradiance from the Sun is $B_{sun} = 1366$ w/m^2 and the solar irradiance in the sensor bandpass is $B_{sun}k_{sun}$. Now apply the visual magnitude scaling equation again to calculate B_0 from scaling the Solar brightness and magnitude,

$$B_0 = B_{sun}k_{sen}10^{0.4\, m_{sun}}$$

Given B_0 , It is now possible to calculate the irradiance of the of the point source on the aperture as $Irr_{sen} = B_0 10^{-0.4 m_v}$. The irradiance signal level propagated through the optics, converted to photons and elections leading to a peak signal in electrons. The signal in electrons is this intensity times the transmission, aperture area, integration time, quantum efficiency, and Ensquared Energy (EE) factor to describe diffraction loss,

$$S_e = Irr_{sen}(A_o)\left(\frac{\lambda}{hc}\right)T_{int}(\tau_o QE)(EE).$$

The EE factor is essentially the peak of the point spread function and is the fractional portion of the total signal that appears in the strongest pixel of the point signature. This is the peak of the signal on the detector from the point source. The EE factor is described as follows:

$$EE = \int_{-0.5}^{0.5}\int_{-0.5}^{0.5} PSF(u,v)\, du\, dv$$

The noise on the detector is calculated by RSS the read noise, shot noise, and dark current,

$$N_e^2 = N_{read}^2 + S_e + I_{dark}T_{int}$$

This signal in electrons is divided by noise to get SNR for detection performance. In summary, the SNR determines the ability to detect the satellite in a single image and the false alarm performance. With Gaussian statistics on the noise, an example detection threshold with an SNR of 4.75 will lead to an expectation of about 1 false alarm in every megapixel of detector area as shown in Fig 5.

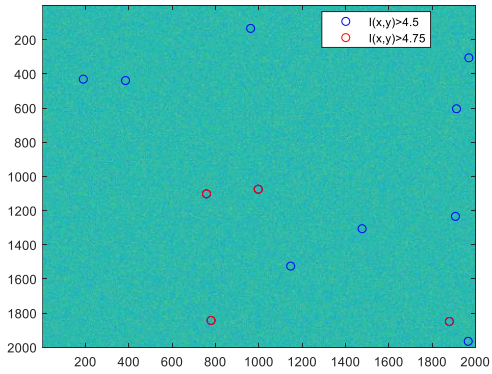

Fig 5. Increasing false alarms with lower SNR threshold. At 4.75 about 1 FA per 1Kx1K image

2.3 ROC analysis for Single and Multiple Images

It is assumed that the observing satellite is pointing towards a target region on the geo-belt and satellites will be relatively stationary compared to the starfield. The starfield is removed by correlating stars in the image in successive collections and satellite objects remain. If detections are required in a low SNR environment, the detection threshold is lowered to allow more detections with increased false alarms. Assuming a Gaussian detector noise model and a fixed SNR on the target, the Receiver Operator Characteristic (ROC) curves showing Probability of detection to false alarm rate are shown in Fig 6.

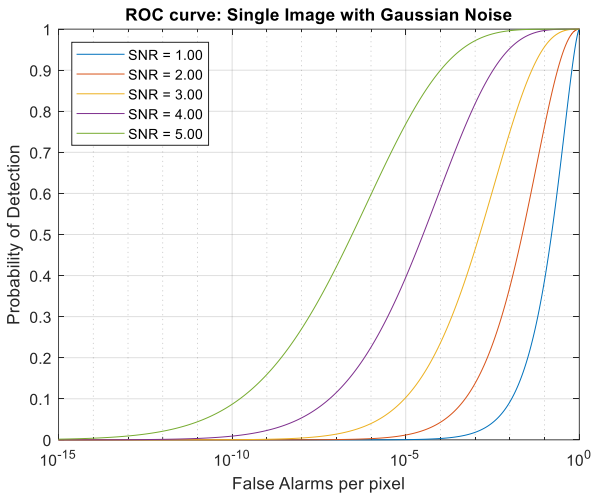

Fig. 6 ROC curves for single detection with Gaussian Noise

The single detection ROC curve is based on a fixed threshold on one sparse image. A notional Track before Detect modelling approach will consider multiple images to improve the detection probability of lower SNR targets. Mathematical approach uses logic that lowers detection threshold to allow lower SNR detections but for single images, allows increased false alarms. The low SNR detections are validated by correlating them in successive frames over the multiple detections. Essentially the detections are correlated in multiple images to verify the true detections and the false alarms are removed.

To mathematically model the detection logic, it is assumed the correlations will occur within a small region or gate between the successive images. To correlate a detection between two images, assume that a detection in the first image is near the location in the second image but some movement is allowed. The second detection must be within a gate of n pixels around the location of the first image. N_{gate} is the number of pixels in the gate of the second neighborhood, The detection probability and false alarm probability when testing within the gate region is as follows,

$$p_{d\,gate} = p_{d1}$$
$$p_{fa\,gate} = 1 - \left(1 - p_{fa1}\right)^{N_{gate}}$$

Now the detection probability is the same since there is assumed on detection between the images so it will only appear once in each image at most. Multiple false alarms are potentially possible since each pixel has independent noise and any individual false alarm in the N_{gate} region will trigger a verified detection false alarm.

This logic can be further extended using a “K out of N” rule. The false alarms can be lowered by requiring the target be present in “K out of N” images which is evaluated using a modified binomial distribution. The lower threshold allows improved detection, correlation, and results in fewer false alarms. It is modelled by taking the image PD and FA and applying the modified binomial distraction. Updated PD and FA for “K out of N” rule.

The approach is to model the contributions of each frame to the detection probability. Refer to Fig. 7 below. Now there are *N* frames and the first detection can occur on the *i*th frame. The first (*i*-1) frames have no detections. There is detection at the *i*th frame. The remaining frames are correlated to the *i*th frame using the correlation gate. This portion will have binomial statistics with *K-1* events in *N-i* trials. This totals to *N* frames and the overall probability is the multiplication of these individual probabilities.

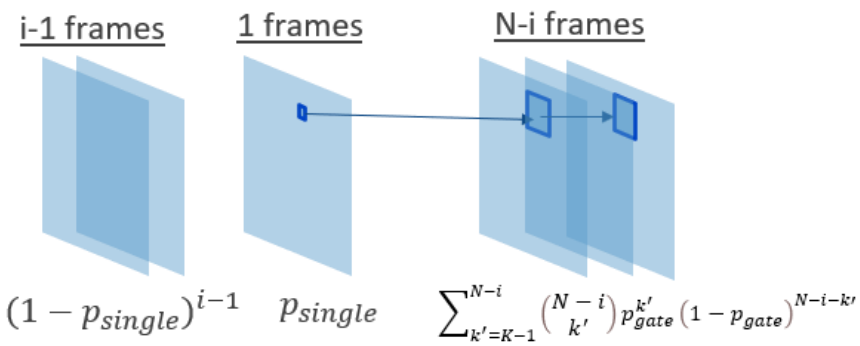

Fig. 7. Contribution of each frame to the total probability

The final detection and false alarm probability result from the sum of *i* from 1 to *N*,

$$p_{dK|N}=\sum_{i=1}^{N-K+1}(1-p_{d1})^{i-1}(p_{d1})\sum_{k'=K-1}^{N-i}\binom{N-i}{k'}p_{d\,gate}^{k'}\left(1-p_{d\,gate}\right)^{N-i-k'}$$
$$p_{faK|N}=\sum_{i=1}^{N-K+1}\left(1-p_{fa1}\right)^{i-1}(p_{fa1})\sum_{k'=K-1}^{N-i}\binom{N-i}{k'}p_{fa\,gate}^{k'}\left(1-p_{fa\,gate}\right)^{N-i-k'}$$

Fig 8 shows a comparison of ROC curves generated from single image detection logic and K of N logic. This assumes Gaussian noise and the signal is present with an SNR of 3.5.

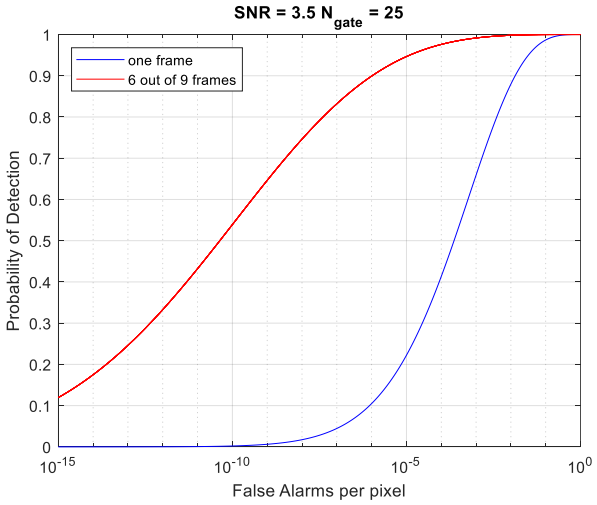

Fig. 8. Predicted detection performance when the SNR is 3.5 and Ngate = 25 (5x5)

The equation allows us to find the detection performance variation as K changes when the number of images is fixed. Here there are 9 image to correlate the detections. Fig 9(a) show plots of how performance varies with K for a signal with SNR of 4. What is interesting is that best performance is when K is about 60% of N. High values of K near 8 and 9 are too restrictive and prevent detection. Low values of K near 1, 2 and 3 cause too many false alarms causing the ROC curve to move to the right. The best performance is when is neither extremely high nor low but closer to 60%.

We can compare detection performance as the number of image collections vary. Fig 9(b) show 3 cases with number of collections as 3, 6, and 9. Here K is 66% of the N for 2 of 3, 4 of 6, and 6 of 9 detection rules. As expected, detection performance improves as the number images increase which is an expected result.

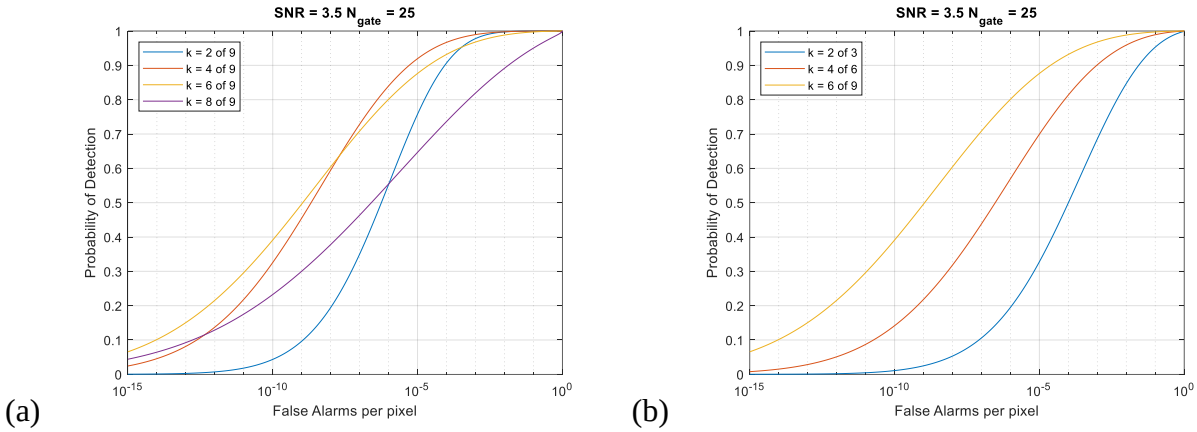

Fig. 9. Predicted detection performance when the SNR is 3.5

2.4 Comparison ROC curves from MATLAB Simulation of Tracker with Global Nearest Neighbor Association

For a more realistic scenario, a simple tracking logic will be used to associate the detections between the images. The tracks are updated by associating current detections to current tracks if they are within the correlation gate. Global Nearest Neighbor association means that closest detection is automatically associated with closest tracks without multi-Hypothesis logic to create extra tracks for other nearby detections in the gate. After association the track position is updated as the mean location of the detections. A false alarm is only counted if there is no valid detections within the track. There is no track deletion logic.

There are 7 images in a sequence and the tracker will need to use a KofN association rule to verify the detection. The images have a has dimensions 1000x1000 and normally distributed noise with zero mean and standard deviation of one, $n_i(x, y) = \mathcal{N}(0,1)$. The image has a target inserted with an SNR of 3.5 and additive gaussian noise. The correlation gate is a 5x5 pixel region with N_{gate}=25 total pixels. There were 10000 trials in the experiment. Fig. 10 shows the results with a simple tracker, and they agree well with the analytic ROC curves.

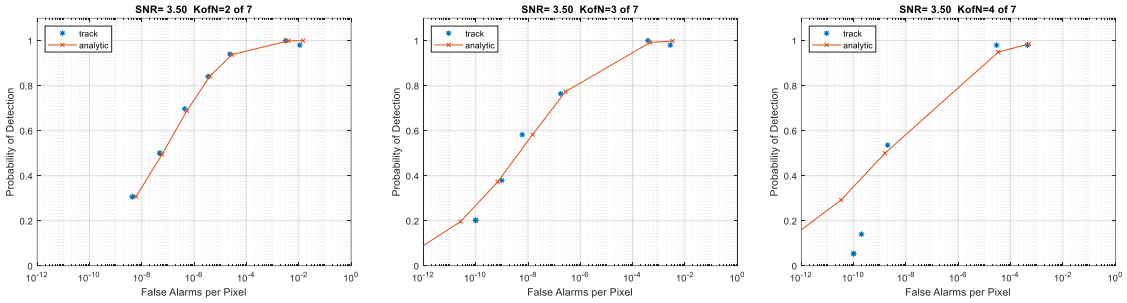

Fig. 10. Comparing modelled KofN ROC curves with MATLAB simulation and GNN tracker

3. DISCUSSION AND CONCLUSIONS

This work provides an equation-based model to generate ROC curves for multi-frame correlation algorithms. It has only a few parameters for a K of N tracking law and the size of the correlation gate. The equation-based method considers telescope optical and sensor parameters, target size, and collection geometry. Based on this an equation is possible to estimate the performance of a telescope system against a target scenario and a particular tracking logic. The target is stationary in this analysis and more investigation is needed to see how to predict tracking performance for moving targets. The gate region can be extended for faster targets but that might show unnecessarily penalized performance.
Also, the results here are shown for Gaussian noise models but can be extended to more realistic noise like spurious responses and Poisson noise.

REFERENCES

[1] S. M. Tonissen and R. J. Evans, "Peformance of dynamic programming techniques for Track-Before-Detect," in IEEE Transactions on Aerospace and Electronic Systems, vol. 32, no. 4, pp. 1440-1451, Oct. 1996, doi: 10.1109/7.543865.
[2] Tagawa, M., Yanagisawa, T., Matsun, H. Hanada, T., "Space-Based Short Range Observations for LEO Debris", Proc. '6th European Conference on Space Debris',Darmstadt, Germany, 22-25 April 2013 (ESA SP-723, August 2013)
[3] "SBSS-DM and ANDROID: two small missions for Space-Based Space Surveillance and Active Debris Removal Demonstrations"
[4] Vallado, D.A., "Evaluating Gooding Angles-only Orbit Determination of Space Based Space Surveillance Measurements", AAS 10-xxx, Born, 2010.
[5] M. Fischler and R. Bolles, "RANdom SAmpling Consensus: a paradigm for model fitting with application to image analysis and automated cartography," in Commun. Assoc. Comp. Mach., June 1981, vol. 24, pp. 381–395.
[6] Hardy, T. J. (2015), "Optical Theory Improvements to Space Domain Awareness", AFIT-ENG-DS-16-S-011, Doctoral Dissertation, Air Force Institute of Technology Wright Patterson AFB
[7] Samuel Blackman, " Multiple Hypothesis Tracking For Multiple Target Tracking", IEEE A&E SYSTEMS MAGAZINE VOL. 19, NO. 1 JANUARY 2004